

Geometric growth and character development in large metastable networks

K. BARMAK – E. EGGELING – M. EMELIANENKO

Y. EPSHTEYN – D. KINDERLEHRER – S. TA'ASAN

ABSTRACT: *Cellular networks are ubiquitous in nature. They exhibit behavior on many different length and time scales and are generally metastable. Most technologically useful materials are polycrystalline microstructures composed of a myriad of small monocrystalline grains separated by grain boundaries. The energetics and connectivity of the grain boundary network plays a crucial role in determining the properties of a material across a wide range of scales. A central problem in materials science is to develop technologies capable of producing an arrangement of grains – a texture – that provides for a desired set of material properties.*

Here we discuss briefly the role of energy in texture development, measured by a character distribution, and how this is different from the evolution of geometric features, which we term geometric coarsening. For this purpose we present a critical event model to deepen our understanding of the topological reconfigurations that occur during the growth process.

1 – Introduction

Most technologically useful materials arise as polycrystalline microstructures, composed of a myriad of small crystallites or grains, the cells, separated by interfaces or grain boundaries. Coarsening consists in the growth and rearrangement of the crystallites, which may be viewed as the anisotropic evolution of a

KEY WORDS AND PHRASES: *Geometric coarsening – Texture development – Critical event model – Free energy – Fokker-Plank equation – Wasserstein metric*

A.M.S. CLASSIFICATION: 37M05, 35Q80, 93E03, 60J60, 35K15, 35A15.

large metastable system. Two processes compete during coarsening in a cellular network. Energy cost tends to reduce the amount of interface in the configuration, while, simultaneously, available space must be filled. As energy decreases, cells increase in size and small cells and interfaces tend to be eliminated in order to maintain the space filling constraint. In a given material system, many other features may interfere with these primary mechanisms, like second phase precipitates, impurities, and dislocation arrays, but here we shall limit ourselves to discussion of the growth process in two dimensions. Although the space filling constraint requires reduction of the number of cells, how this transpires depends on properties of the energy itself. This distinguishes one material from another. It is the main topic of our investigation and here we wish to discuss some first thoughts.

In simulation [18] we are presented with thousands of coupled nonlinear partial differential equations representing details of the evolution. Assorted statistics may be harvested and suggested as material properties. But we lack a theory to predict or to verify the reliability of such statistics. In general, these multiscale processes require “upscaling” or “coarse graining” for interpretation and subsequent predictive capability. Our approach here is to investigate some simulation statistics, which we believe to be robust, in conjunction with some ideas of analysis, looking for insight about mesoscale coarsening behavior.

The most straightforward way to measure coarsening is to maintain a record of the average size of cells or the average sizes of cells with a given number of facets. We refer to this aspect of the process as geometric growth.

Texture is characterized at the mesoscale level by geometry and crystallography. This is connected to the preparation of arrangements of grains and boundaries suitable for a dedicated application, a central issue of materials science: it is the problem of microstructure [24]. A fundamental result is that this is an energy dependent material property and not some random feature of a configuration. We introduce the grain boundary character distribution, the GBCD, a basic texture measure, [17], and outline a possible theory for it. For this, a simplified critical event model is introduced. A detailed presentation of the theory appears in [2]. In summary there are two aspects of coarsening, geometric growth and texture development. The main objective of this note is to show that they may be decoupled and characterized by different types of evolution processes, leading to statistically different types of coarsening rates.

There are many coarsening systems, or models of physical systems which undergo an evolution process where coarsening occurs. These run a gamut from Monte Carlo and Potts models to kinetic theory. A number of these display behavior similar to the one we present here and thus we suspect some interesting universal properties. A different critical event model which originates in the Carnegie Mellon MRSEC is found in [26]. We are pleased to acknowledge the collaboration of G. S. Rohrer, A. D. Rollett, and R. Sharp.

2 – Recapitulation of mesoscale theory

There is a common denominator theory for the mesoscale description of microstructural evolution. This is growth by curvature, the Mullins Equation (2.2) below, for the evolution of curves or arcs individually or in a network. Boundary conditions must be imposed where the arcs meet. This condition is the Herring Condition, (2.3), which is the natural boundary condition at equilibrium for the Mullins Equation. Since their introduction by Mullins, [22], and Herring, [13], [14], a large and distinguished body of work has grown about these equations. Most relevant to here are [11], [8], [16], [23]. Let α denote the misorientation between two grains separated by an arc Γ , as noted in Figure 1, with normal $n = (\cos \theta, \sin \theta)$, tangent direction b and curvature κ . Let $\psi = \psi(\theta, \alpha)$ denote the energy density on Γ . So

$$(2.1) \quad \Gamma : x = \xi(s, t), \quad 0 \leq s \leq L, \quad t > 0,$$

with

$$b = \frac{\partial \xi}{\partial s} \text{ (tangent) and } n = Rb \text{ (normal)}$$

$$v = \frac{\partial \xi}{\partial t} \text{ (velocity) and } v_n = v \cdot n \text{ (normal velocity)}$$

where R is a positive rotation of $\pi/2$. The Mullins Equation of evolution is

$$(2.2) \quad v_n = (\psi_{\theta\theta} + \psi)\kappa \text{ on } \Gamma.$$

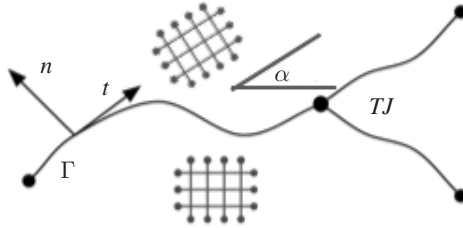


Fig. 1: An arc Γ with normal n , tangent t , and lattice misorientation α , illustrating lattice elements.

We assume that only triple junctions are stable and that the Herring Condition holds at triple junctions. This means that whenever three curves $\{\Gamma^{(1)}, \Gamma^{(2)}, \Gamma^{(3)}\}$, meet at a point p the force balance, (2.3) below, holds:

$$(2.3) \quad \sum_{i=1, \dots, 3} (\psi_{\theta} n^{(i)} + \psi b^{(i)}) = 0.$$

It is easy to check that the instantaneous rate of change of energy of Γ is

$$(2.4) \quad \frac{d}{dt} \int_{\Gamma} \psi |b| ds = - \int_{\Gamma} v_n^2 ds + v \cdot (\psi_{\theta} n + \psi b)|_{\partial \Gamma}.$$

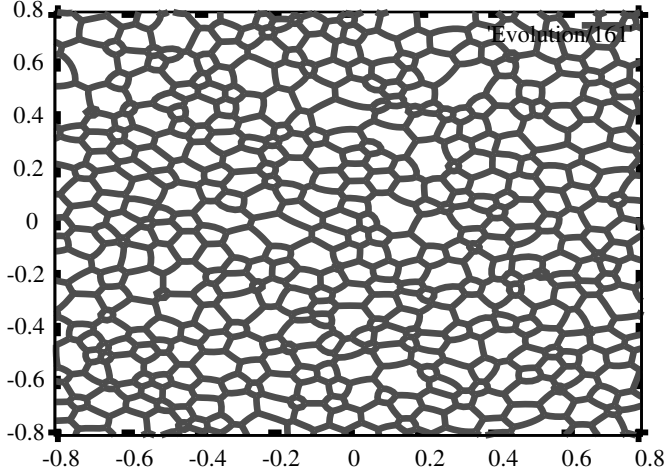


Fig. 2: Example of a cellular network from simulation. This is from a small simulation with constant energy density and periodic conditions at the border of the configuration.

We turn now to a network of grains bounded by $\{\Gamma_i\}$ subject to some condition at the border of the region they occupy, like fixed end points or periodicity, *cf.* Figure 2. The typical simulation consists in initializing a configuration of cells and their boundary arcs, usually by a modified Voronoi tessellation, and solving the system (2.2), (2.3), eliminating facets when they have negligible length and cells when they have negligible area. The total energy of the system is given by

$$(2.5) \quad E(t) = \sum_{\{\Gamma_i\}} \psi |b| ds.$$

Owing exactly to the Herring Condition (2.3), the instantaneous rate of change of the energy

$$(2.6) \quad \begin{aligned} \frac{d}{dt} E(t) &= - \sum_{\{\Gamma_i\}} \int_{\Gamma_i} v_n^2 ds + \sum_{TJ} v \cdot \sum (\psi_{\theta} n + \psi b) = \\ &= - \sum_{\{\Gamma_i\}} \int_{\Gamma_i} v_n^2 ds \leq \\ &\leq 0, \end{aligned}$$

rendering the network dissipative for the energy in any instant absent of critical events. Indeed, in an interval $(t_0, t_0 + \tau)$ where there are no critical events, we may integrate (2.6) to obtain a local dissipation equation

$$(2.7) \quad \sum_{\{\Gamma_i\}} \int_{t_0}^{t_0+\tau} \int_{\Gamma_i} v_n^2 ds dt + E(t_0 + \tau) = E(t_0)$$

which bears a strong resemblance to the simple dissipation relation for an ensemble of inertia free springs with friction. In the simulation, the facet interchange and cell deletion are arranged so that (2.6) is maintained. Suppose, for simplicity, that the energy density is independent of the normal direction, so $\psi = \psi(\alpha)$. Then (2.2) and (2.3) may be expressed

$$(2.8) \quad v_n = \psi \kappa \text{ on } \Gamma$$

$$(2.9) \quad \sum_{i=1, \dots, 3} \psi b^{(i)} = 0 \text{ at } p,$$

where p denotes a triple junction. (2.9) is the same as the Young wetting law. For this situation we define the grain boundary character distribution, GBCD,

$\rho(\alpha, t)$ = relative length of arc of misorientation α at time t ,

$$(2.10) \quad \text{normalized so that } \int_{\Omega} \rho d\alpha = 1.$$

For consistency, in this note all computational results are drawn from a single run initially of 10^3 cells with cell orientations distributed normally.

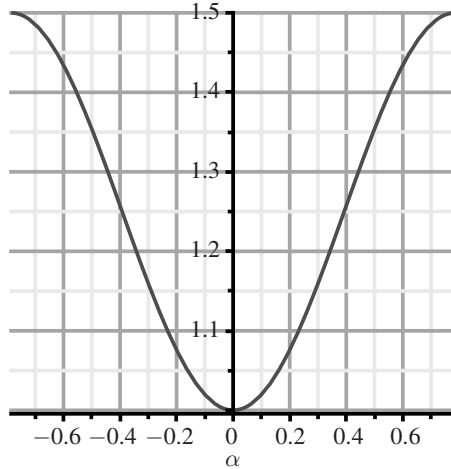


Fig. 3: The energy density $\psi(\alpha) = 1 + \epsilon \sin^2 2\alpha$, $\epsilon = \frac{1}{2}$, used for the examples in this note.

3 – Geometric coarsening

In this note we attempt to explain properties of texture. In order to compare with geometric growth, we here make a brief excursion. For an individual cell in an ensemble with constant facet energy density, (2.2) and (2.3) lead to the well known von Neumann-Mullins $n - 6$ rule, [28], [21]: the rate of change of area of an n -faceted cell with constant surface energy and exterior angles meeting at $2\pi/3$ is proportional to $n - 6$, *i.e.*,

$$(3.1) \quad \frac{dA_n}{dt} = c(n - 6), \text{ where } A_n \text{ is the area of an } n\text{-faceted cell}$$

and $c > 0$ is some material constant. It is often thought, on this basis, that the average cell area $A(t)$ should be an affine function of t . This is in fact true in our simulations, *cf.* Figure 4(a), but it depends in a complicated way on the initialization. It sometimes holds in experiment. The essential property here is that geometric growth tends to behave like transport, as indeed suggested by (3.1), and is highly dependent on initial conditions. There are a number of papers which discuss this, including two new works [9] and [12], and [6], where additional references may be found. The very recent n -dimensional extension of (3.1) is given in [20].

An elementary argument suggests how total energy (2.5) decays. The energy of coarsening should be proportional to the total length of arc $L(t)$ in the configuration which is approximately the average perimeter $= \sqrt{A(t)}$ times the number of cells $N(t) = 1/A(t)$, or

$$(3.2) \quad \begin{aligned} L(t) &\approx \sqrt{A(t)} \cdot N(t) = \\ &= \frac{1}{\sqrt{A(t)}} = \\ &= \frac{1}{\sqrt{A_0 + A_1 t}}. \end{aligned}$$

For this simple reason, there is a long tail distribution for energy decay.

4 – Simplified critical event model

Inspection of Figure 4(b) shows that contrary to (3.1), the average area of five sided grains during a growth experiment on an *Al* thin film increases several-fold during coarsening. (3.1) does not fail but most of the grains observed at time $t = 2$ hours, for example, had 6, 7, 8, ... sides at some earlier time $t < 2$ hours. Thus in the network setting, the topological changes play a major role. Although we may be reasonably confident that small cells with small numbers of facets will be deleted, their effect on the configuration is essentially random.

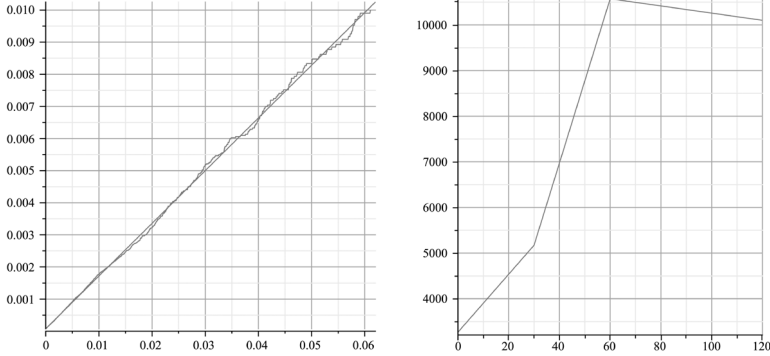


Fig. 4: (a) Simulations tend to exhibit linear average growth in area. (b) Average area in nm^2 of five sided grains in an Al columnar grain structure increases (time in minutes) in distinction to the von Neumann-Mullins (3.1) rule valid for single cells.

A significant difficulty in developing a theory of the GBCD, and understanding texture development in general, lies in the lack of understanding of the relationship between these stochastic or critical events and the system energy. This leads us to a reduced model, which is a critical event model. This is a system of cells on a line segment. Each cell is an interval with a given misorientation parameter subject to nearest neighbor interactions. We have used this system to develop a statistical theory for critical events in [3], [4], [5]. Can it also be employed to study the GBCD directly? We address this briefly here. Consider a partition of a circle of circumference $L > 0$ by n randomly chosen points, equivalently a partition of the interval $[0, L] \subset \mathbf{R}$ by points $x_i, i = 1 \dots n$, where $x_i < x_{i+1}, i = 1 \dots n - 1$ and x_{n+1} identified with x_1 . For each interval $[x_i, x_{i+1}], i = 1 \dots, n$ select a random misorientation number $\alpha_i \in \mathbf{R}$. The intervals $[x_i, x_{i+1}]$ correspond to cells and the points x_i represent the triple junctions. Choose an energy density $\psi(\alpha)$ and define the energy

$$(4.1) \quad E = \sum_{i=1 \dots n} \psi(\alpha_i)(x_{i+1} - x_i).$$

We impose gradient flow kinetics with respect to (4.1), which is the system of ordinary differential equations

$$(4.2) \quad \frac{dx_i}{dt} = \psi(\alpha_i) - \psi(\alpha_{i-1}), i = 2 \dots n, \text{ and } \frac{dx_1}{dt} = \psi(\alpha_1) - \psi(\alpha_n).$$

The velocity v_i of the i^{th} boundary is

$$(4.3) \quad v_i = \frac{dx_{i+1}}{dt} - \frac{dx_i}{dt} = \psi(\alpha_{i-1}) - 2\psi(\alpha_i) + \psi(\alpha_{i+1}).$$

The grain boundary velocities are constant until one of the boundaries collapses. That segment is removed from the list of current grain boundaries and the velocities of its two neighbors are changed due to the emergence of a new junction. Each such deletion event rearranges the network and, therefore, affects its subsequent evolution just as in the two dimensional cellular network.

There is also a dissipation inequality for this gradient flow. At any time t between deletion events,

$$\begin{aligned}
 (4.4) \quad \frac{dE}{dt} &= \sum \psi(\alpha_i) v_i = \\
 &= - \sum (\psi(\alpha_i) - \psi(\alpha_{i-1}))^2 = \\
 &= - \sum \frac{dx_i^2}{dt}.
 \end{aligned}$$

Moreover, if the segment $[x_c, x_{c+1}]$ is deleted at at time t_0 then $v_c < 0$ for $t < t_0$. This may be used to show that

$$E(t_0) \leq \lim_{t \rightarrow t_0} E(t),$$

as discussed in [3], [4], [5]. Likewise we may write a spring-like local dissipation equation analogous to (2.7), thanks to (4.4). In an interval $(t_0, t_0 + \tau)$ where there are no critical events, (4.4) may be integrated to give

$$\tau \sum_{i=1 \dots n} \frac{dx_i^2}{dt} + E(t_0 + \tau) = E(t_0)$$

or

$$(4.5) \quad \sum_{i=1 \dots n} \int_0^\tau \frac{dx_i^2}{dt} dt + E(t_0 + \tau) = E(t_0).$$

With the obvious use of Young's Inequality, we have that

$$(4.6) \quad \frac{1}{4} \sum_{i=1 \dots n} \int_0^\tau v_i^2 dt + E(t_0 + \tau) \leq E(t_0).$$

The energy of the system at time $t_0 + \tau$ is determined by its state at time t_0 . Vice versa, changing the sign on the right hand side of (4.2) allows us to begin with the state at time $t_0 + \tau$ and return to the state of time t_0 : the system is reversible in an interval of time absent of critical events. This is no longer the situation after a critical event. At the later time, we have no knowledge about which interval, now no longer in the inventory, was deleted.

We introduce a new ensemble based on the misorientation parameter α where we take $\Omega : -\frac{\pi}{4} \leq \alpha \leq \frac{\pi}{4}$, for later ease of comparison with the two dimensional network for which we are imposing ‘‘cubic’’ symmetry, *i.e.*, ‘‘square’’ symmetry in the plane. The *GBCD* or character distribution in this context is, as expected, the histogram of lengths of intervals sorted by misorientation α scaled to be a probability distribution on Ω . To be precise, let

$$\begin{aligned} l_i(\alpha, t) &= x_{i+1}(t) - x_i(t) = \\ &= \text{length of the } i^{\text{th}} \text{ interval, where explicit note has been taken of} \\ &\quad \text{its misorientation parameter } \alpha. \end{aligned}$$

Now partition Ω into m subintervals of length $h = \frac{\pi}{2} \frac{1}{m}$ and let

$$(4.7) \quad \rho(\alpha, t) = \sum_{\alpha' \in ((k-1)h, kh]} l_i(\alpha', t) \cdot \frac{1}{Lh}, \text{ for } (k-1)h < \alpha \leq kh.$$

We may express (4.6) in terms of the character distribution (4.7). After some manipulations, this amounts to

$$(4.8) \quad \begin{aligned} \mu_0 \int_{t_0}^{t_0+\tau} \sum_k \frac{\partial \rho}{\partial t}(\hat{\alpha}_k, t)^2 h dt + \sum_k \psi(\hat{\alpha}_k) \rho(\hat{\alpha}_k, t_0 + \tau) h &\leq \\ &\leq \sum_k \psi((\hat{\alpha}_k) \rho((\hat{\alpha}_k, t_0) h, \end{aligned}$$

or, at this point passing to a continuous limit for ease of discussion,

$$(4.9) \quad \mu_0 \int_{t_0}^{t_0+\tau} \int_{\Omega} \frac{\partial \rho}{\partial t}(\alpha, t)^2 d\alpha dt + \int_{\Omega} \psi(\alpha) \rho(\alpha, t_0 + \tau) d\alpha \leq \int_{\Omega} \psi(\alpha) \rho(\alpha, t_0) d\alpha,$$

where $\mu_0 > 0$ is some constant. We now impose a modeling assumption. The expression (4.9) is at a larger scale, the misorientation scale, than the original system and, consistent with the lack of reversibility as critical events occur, an entropic term will be added. We use the standard configurational entropy, although this is not the only choice. It is

$$(4.10) \quad + \int_{\Omega} \rho \log \rho d\alpha,$$

which is minus the usual physical entropy. Minimizing (4.10) favors the uniform state, which would be our situation were $\psi(\alpha) = \text{constant}$.

Knowing that (4.9) holds in any interval where no critical events occur, we assume that for any t_0, τ

$$(4.11) \quad \begin{aligned} \mu_0 \int_{t_0}^{t_0+\tau} \int_{\Omega} \left(\frac{\partial \rho}{\partial t} \right)^2 d\alpha dt + \int_{\Omega} (\psi \rho + \lambda \rho \log \rho) d\alpha |_{t_0+\tau} &\leq \\ &\leq \int_{\Omega} (\psi \rho + \lambda \rho \log \rho) d\alpha |_{t_0}. \end{aligned}$$

$E(t)$ was analogous to an internal energy or the energy of a microcanonical ensemble and now

$$(4.12) \quad F(t) = F_\lambda(t) = E(t) + \lambda \int_{\Omega} \rho \log \rho d\alpha$$

is a free energy. This type of reasoning differs from conventional thermodynamic thinking in two respects. First, the ensembles are not molecules or idealized quantities like spins, but segments and, in the case of the full two dimensional network, curves. Second, this is not an equilibrium situation based on Hamiltonian systems but a kinetic non-equilibrium process based on a dissipation principle. More explanation is given in [2], as noted in the introduction.

Is there an optimal choice of the “temperature” parameter λ and how would we determine it? Is there one at all? We bring (4.11) to a different form by observing that the first term on the left dominates, with a system dependent factor, the conventional Wasserstein-2 metric, [25], [27], [1], or the square of the Wasserstein-1 metric. (We thank Adrian Tudorascu for his help on these points.) Denote this metric by d ; a definition is given in the Appendix. Let $\rho^*(\alpha) = \rho(\alpha, t_0)$ and $\rho(\alpha) = \rho(\alpha, t_0 + \tau)$. We then have that

$$(4.13) \quad \frac{\mu}{2\tau} d(\rho, \rho^*)^2 + F_\lambda(\rho) \leq F_\lambda(\rho^*),$$

which resembles the Wasserstein metric implicit scheme. Here is the scheme. Suppose that u is the limit as $\tau \rightarrow 0$ of a sequence of iterates $\{u^{(\tau, k)}\}$ that satisfy

$$(4.14) \quad \frac{1}{2\tau} d(u^{(\tau, k)}, u^{(\tau, k-1)})^2 + F_\sigma(u^{(\tau, k)}) = \min_v \left(\frac{1}{2\tau} d(v, u^{(\tau, k-1)})^2 + F_\sigma(v) \right),$$

$$\int_{\Omega} v d\alpha = 1 \text{ and } v \geq 0 \text{ in } \Omega.$$

We then know that u is a solution of the Fokker-Planck Equation

$$(4.15) \quad \frac{\partial u}{\partial t} = \frac{\partial}{\partial \alpha} \left(\sigma \frac{\partial u}{\partial \alpha} + \psi' u \right) \text{ in } \Omega, \quad 0 < t < \infty$$

with, in this situation, periodic boundary conditions, [15]. We do not know if our $\rho(\alpha, t)$ is a solution of (4.15) but we may ask if characterizations of u may assist in identifying the parameter σ and if there are desirable properties of u which are also shared by ρ .

First note that a solution u of (4.15) tends to the stationary solution with appropriate mass, in this case, the Boltzmann distribution for ψ with unit mass,

$$(4.16) \quad u \rightarrow \rho_\sigma \text{ as } t \rightarrow \infty,$$

where

$$(4.17) \quad \rho_\lambda(\alpha) = \frac{1}{Z_\lambda} e^{-\frac{\psi(\alpha)}{\lambda}}, \quad Z_\lambda = \int_{\Omega} e^{-\frac{\psi(x)}{\lambda}} dx.$$

Recall that the Kullback-Liebler relative entropy for the Fokker-Planck Equation is given by

$$(4.18) \quad \begin{aligned} \Phi_\lambda(v) &= \int_{\Omega} v \log \frac{v}{\rho_\lambda} d\alpha, \text{ and} \\ \Phi_\lambda(v) &= F_\lambda(v) + \lambda \log Z_\lambda, \end{aligned}$$

where v is a probability density on Ω . By Jensen's Inequality,

$$(4.19) \quad \Phi_\lambda(v) \geq 0,$$

and thus according to (4.16),

$$(4.20) \quad \begin{aligned} \Phi_\sigma(u) &\geq 0 \text{ and } \Phi_\sigma(u) \rightarrow 0 \text{ as } t \rightarrow 0 \text{ whereas} \\ \Phi_\lambda(u) &\rightarrow \text{a positive function of } \alpha \text{ for } \lambda \neq \sigma. \end{aligned}$$

Our GBCD (4.7) always satisfies (4.19), so we may attempt to use (4.20) to identify the diffusion coefficient σ , simply by inspection. An equivalent more colorful approach is to compare the plots of $\{F_\lambda(\rho)\}$ as functions of t and ask for the largest one which is decreasing. To check whether or not this makes any sense, we then compare the empirical ρ with ρ_σ . Figure 5 shows that we may indeed identify the solution by this procedure. Let us keep in mind here that we are not writing of solutions of partial differential equations. We are seeking a property of a statistic of a simulation. We thus interpret our result as validation of (4.11) and (4.13). For solutions u of (4.15), the relative entropy decays exponentially, namely

$$(4.21) \quad \Phi_\sigma(u)(t) \leq C e^{-rt}, \text{ for some } C > 0, r > 0,$$

which can be checked by calculating the derivative of $\Phi_\sigma(u)(t)$ and then applying the log-Sobolev inequality and the Gronwall lemma. We may, additionally, verify exponential convergence of the energy or free energy of u by application of the Csiszar-Kullback Inequality [19],

$$(4.22) \quad \left(\int_{\Omega} |f - f^\dagger| dx \right)^2 \leq 2 \int_{\Omega} f \log \frac{f}{f^\dagger} dx, \text{ for probability densities } f, f^\dagger.$$

Applying this in an obvious way to u , we obtain that

$$(4.23) \quad \left| \int_{\Omega} \psi u(\alpha, t) d\alpha - \int_{\Omega} \psi \rho_\sigma(\alpha) d\alpha \right| \leq C_0 e^{-\frac{r}{2}t}.$$

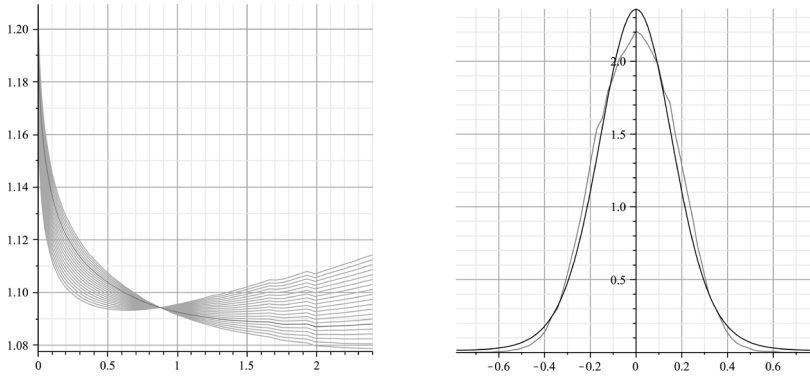


Fig. 5: (a) The free energy (4.12) of the critical event model for a sequence of λ with the optimal choice σ noted. (b) Comparison of the empirical distribution of the critical event model at time $t = 1$ with ρ_σ of (4.17).

Now the application here of (4.22) depends only on the decay property (4.21) of the relative entropy and not on the fact that u is a solution of (4.15), so we may apply this to the statistic as well. Exponential decay of the free energy, and hence the relative entropy, holds for ρ (not shown because of space limitations). Thus we may deduce from (4.22) that

$$(4.24) \quad \left| \int_{\Omega} \psi \rho(\alpha, t) d\alpha - \int_{\Omega} \psi \rho_\sigma(\alpha) d\alpha \right| \leq C_0 e^{-\frac{r}{2}t}.$$

We may summarize these considerations by writing that the GBCD for the reduced critical event model is, in essence, the solution of a Fokker-Planck Equation for a long intermediate period of its lifetime.

5 – Microstructural coarsening

The local dissipation equation (2.7) does not lead to an implicit scheme for the GBCD of the two dimensional evolution system, at least not known to us at this point of our development. We may, nonetheless, attempt to choose the correct variance parameter σ by the same method as above and to then validate it, if possible, by comparison between the empirical GBCD and the associated ρ_σ . In Figure 6 we see the result of this exercise. Indeed, the kinetics of the GBCD are indistinguishable from those of the critical event model. Astonishingly, the parameter σ is identical for our test ψ , Figure 3. The quantity

$$\frac{\sigma}{\epsilon}$$

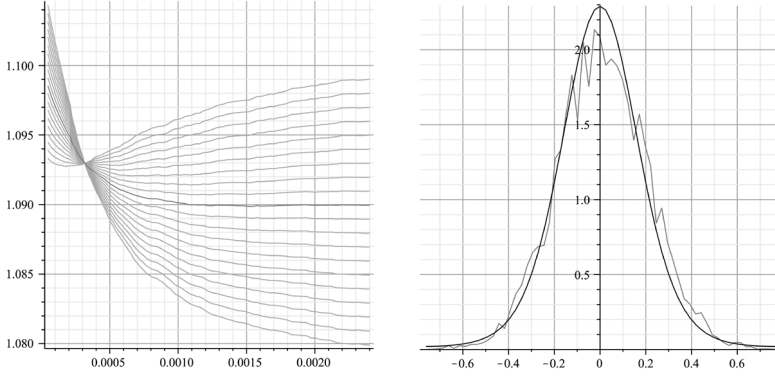


Fig. 6: (a) The free energy (4.12) of the grain growth simulation for a sequence of λ with the optimal choice σ noted. (b) Comparison of the empirical distribution at time $t = 0.0015$ with ρ_σ of (4.17).

is invariant of choice of ϵ in the simulation. Although obvious for the reduced critical event model, it is not clear why this property holds for the large scale simulation. In Figure 7(a), we plot $-\log(\Phi_\sigma(\rho)(t))$ vs. t illustrating approximate linear growth to a level where it remains stationary. Thus the relative entropy Φ_σ decays exponentially.

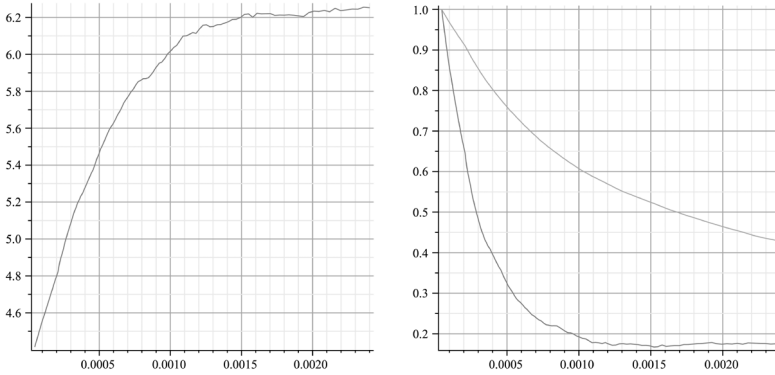


Fig. 7: (a) Plot of $-\log(\Phi_\sigma(\rho)(t))$ vs. t of the GBCD showing that it increases to stationarity approximately linearly. (b) Plots of the geometric coarsening $L(t)$, illustrating its long tail distribution (upper plot), and the relative entropy $\Phi_\sigma(\rho)(t)$ of the GBCD, illustrating exponential decay (lower plot), with time.

Arguing as in the previous section, the Csizar-Kullback Inequality then gives, analogous to (4.24), that

$$(5.1) \quad \left| \int_{\Omega} \psi\rho(\alpha, t)d\alpha - \int_{\Omega} \psi\rho_\sigma(\alpha)d\alpha \right| \leq C_0 e^{-st} \text{ for some } s > 0,$$

where $\rho(\alpha, t)$ defined by (2.10) is the empirical GBCD determined by the simulation. In Figure 7(b), we plot the total length of arc in the simulation $L(t)$ and the relative entropy $\Phi_\sigma(\rho)(t)$ normalized by their values at $t = 0$, namely,

$$\frac{L(t)}{L(0)} \text{ and } \frac{\Phi_\sigma(\rho)(t)}{\Phi_\sigma(\rho)(0)},$$

illustrating the long tail distribution associated to geometric coarsening and the diffusive exponential decay associated to the GBCD. Not shown is the plot showing that $L(t)^{-2}$ is a linear function, as suggested by (3.2) and Figure 4(b).

6 – Appendix: the Monge-Kantorovich-Wasserstein metric

We briefly review the notion of Wasserstein metric used in to implement the implicit scheme (4.13) and (4.14). There are many references for this [27], [1]. Let $D \subset \mathbf{R}$ be an interval, perhaps infinite, and f^*, f a pair of probability densities on D (with finite variance). The Wasserstein metric or 2-Wasserstein metric is defined to be

$$(6.1) \quad d(f, f^*)^2 = \inf_P \int_D |x - y|^2 dp(x, y)$$

$P = \text{joint distributions for } f, f^* \text{ on } \bar{D} \times \bar{D},$

i.e., the marginals of any $p \in P$ are f, f^* . The metric induces the weak-* topology on $C(\bar{D})'$. If f, f^* are strictly positive, there is a transfer map which realizes p , essentially the solution of the Monge-Kantorovich mass transfer problem for this situation. This means that there is a strictly increasing

$$(6.2) \quad \begin{aligned} \phi : D &\rightarrow D \text{ such that} \\ \int_D \zeta(y) f(y) dy &= \int_D \zeta(\phi(x)) f^*(x) dx, \quad \zeta \in C(\bar{D}), \text{ and} \\ d(f, f^*)^2 &= \int_D |x - \phi(x)|^2 f^* dx. \end{aligned}$$

It turns out, as was known to Frechét, [10], that in this one dimensional situation,

$$(6.3) \quad \begin{aligned} \phi(x) &= F^{*-1}(F(x)), \quad x \in D, \text{ where} \\ F^*(x) &= \int_{-\infty}^x f^*(x') dx' \text{ and } F(x) = \int_{-\infty}^x f(x') dx' \end{aligned}$$

are the distribution functions of f^*, f . In one dimension there is only one transfer map. Finally, by a result of Benamou and Brenier [7],

$$(6.4) \quad \begin{aligned} \frac{1}{\tau} d(f, f^*)^2 &= \inf \int_0^\tau \int_D v^2 f d\xi dt \\ \text{over deformation paths } &f(\xi, t) \text{ subject to} \\ f_t + (vf)_\xi &= 0, \text{ (continuity equation)} \\ f(\xi, 0) = f^*(\xi), &f(\xi, \tau) = f(\xi) \text{ (initial and terminal conditions).} \end{aligned}$$

The conditions (6.4) are in “Eulerian” form. Likewise there is the “Lagrangian” form which follows by rewriting (6.4) using the transfer function formulation in (6.2),

$$(6.5) \quad \frac{1}{\tau} d(f, f^*)^2 = \inf \int_0^\tau \int_D \phi_t^2 f^* dx$$

over transfer paths $\phi(x, t)$ from D to D with
 $\phi(x, 0) = x$ and $\phi(x, \tau) = \phi(x)$.

We use the representation (6.3) in (6.5) to calculate that for some $c_0 > 0$,

$$(6.6) \quad \frac{1}{\tau} d(\rho, \rho^*)^2 \leq c_0 \int_\Omega \frac{\alpha}{\rho^*(\alpha)} d\alpha \int_{t_0}^{t_0+\tau} \int_\Omega \frac{\partial \rho}{\partial t}(\alpha, t)^2 d\alpha dt,$$

$\rho^*(\alpha) = \rho(\alpha, t_0)$ and $\rho(\alpha) = \rho(\alpha, t_0 + \tau)$.

A known property of the iteration procedure in (4.14) is that iterates remain positive, indeed, bounded below, if the initial data is positive. Thus we are led to (4.13).

Acknowledgement

Research supported by NSF DMR0520425, DMS 0405343, DMS 0305794, DMS 0806703, DMS 0635983.

REFERENCES

- [1] L. AMBROSIO – N. GIGLI – G. SAVARÉ: *Gradient flows in metric spaces and in the space of probability measures*, Lectures in Mathematics ETH Zürich. Birkhäuser Verlag, Basel, second edition, 2008.
- [2] K. BARMAK – E. EGGELING – M. EMELIANENKO – Y. EPSHTEYN – D. KINDERLEHRER – S. TA’ASAN: *A theory of microstructural texture evolution*, 2008.
- [3] K. BARMAK – M. EMELIANENKO – D. GOLOVATY – D. KINDERLEHRER – S. TA’ASAN: *On a statistical theory of critical events in microstructural evolution*, Proceedings of 11th International Symposium on Continuum Models and Discrete Systems, Paris, 2007.
- [4] K. BARMAK – M. EMELIANENKO – D. GOLOVATY – D. KINDERLEHRER – S. TA’ASAN: *A new perspective on texture evolution*, International Journal on Numerical Analysis and Modeling, **5** (2008), 93–108.
- [5] K. BARMAK – M. EMELIANENKO – D. GOLOVATY – D. KINDERLEHRER – S. TA’ASAN: *Towards a statistical theory of texture evolution in polycrystals*, SIAM J. Sci. Comp., **30** (2008), 3150–3169.
- [6] K. BARMAK – D. KINDERLEHRER – I. LIVSHITS – S. TA’ASAN: *Remarks on a multiscale approach to grain growth in polycrystals*, in: *Variational problems in*

- materials science*, volume 68 of Progr. Nonlinear Differential Equations Appl., pages 1-11. Birkhäuser, Basel, 2006.
- [7] J.-D. BENAMOU – Y. BRENIER: *A computational fluid mechanics solution to the Monge-Kantorovich mass transfer problem*, Numer. Math., **84** (2000), 375–393.
- [8] L. BRONSARD – F. REITICH: *On three-phase boundary motion and the singular limit of a vector-valued Ginzburg-Landau equation*, Arch. Rational Mech. Anal., **124** (1993), 355–379.
- [9] A. COHEN: *A probabilistic analysis of two dimensional grain growth*, Ph.D Thesis, Carnegie Mellon University, 2007.
- [10] M. FRECHET: *Sur la distance de deux lois de probabilité*, Comptes Rendus de l'Académie des Sciences Serie I-Mathématique, **244** (1957), 689–692.
- [11] M. GURTIN: *Thermomechanics of evolving phase boundaries in the plane*, Oxford, 1993.
- [12] R. HENSELER – M. HERMANN – B. NIETHAMMER – J.L.L. VELÁZQUEZ: *A kinetic model for grain growth*, (to appear).
- [13] C. HERRING: *Surface tension as a motivation for sintering*, in: *The Physics of Powder Metallurgy*, E. Walter Kingston, editor, pages 143-179, Mcgraw-Hill, New York, 1951.
- [14] C. HERRING: *The use of classical macroscopic concepts in surface energy problems*, in: *Structure and Properties of Solid Surfaces*, Robert Gomer and Cyril Stanley Smith, editors, pages 5-81, Chicago, 1952, the University of Chicago Press. Proceedings of a conference arranged by the National Research Council and held in September, 1952, in Lake Geneva, Wisconsin, USA.
- [15] R. JORDAN – D. KINDERLEHRER – F. OTTO: *The variational formulation of the Fokker-Planck equation*, Siam Journal on Mathematical Analysis, **29** (1998), 1–17.
- [16] D. KINDERLEHRER – C. LIU: *Evolution of grain boundaries*, Mathematical Models and Methods in Applied Sciences, **11** (2001), 713–729.
- [17] D. KINDERLEHRER – I. LIVSHITS – G.S. ROHRER – S. TA'ASAN – P. YU: *Mesoscale simulation of the evolution of the grain boundary character distribution*, Recrystallization and grain growth, pts 1 and 2, **1-2** (2004), 467–470, 1063–1068.
- [18] D. KINDERLEHRER – I. LIVSHITS – S. TA'ASAN: *A variational approach to modeling and simulation of grain growth*, Siam Journal on Scientific computing, **28** (2006), 1694-1715.
- [19] S. KULLBACK: *Information theory and statistics*, Dover Publications Inc., Mineola, NY, 1997. Reprint of the second edition 1968.
- [20] R. D. MACPHERSON – D. J. SROLOVITZ: *The von Neumann relation generalized to coarsening of three-dimensional microstructures*, Nature, **446** (2007), 1053–1055.
- [21] W. W. MULLINS: *2-Dimensional motion of idealized grain growth*, Journal Applied Physics, **27** (1956), 900–904.
- [22] W. W. MULLINS: *Solid Surface Morphologies Governed by Capillarity*, American Society for Metals, Metals Park, Ohio, 1963, 17–66.
- [23] W. W. MULLINS: *On idealized 2-dimensional grain growth*, Scripta Metallurgica, **22** SEP (1988), 1441–1444.

- [24] W. W. MULLINS: *Remarks on the evolution of materials science*, Mrs Bulletin, **21** (1996), 20–27.
- [25] F. OTTO: *Dynamics of labyrinthine pattern formation in magnetic fluids: A mean-field theory*, Archive for Rational Mechanics and Analysis, **141** (1998), 63–103.
- [26] G. S. ROHRER – J. GRUBER – A. D. ROLLETT: *A model for the origin of anisotropic grain boundary character distributions in polycrystalline materials*, Applications of Texture Analysis, Ceram. Trans. 201, Westerville, OH, 2008.
- [27] C. VILLANI: *Topics in optimal transportation of Graduate Studies in Mathematics*, American Mathematical Society, Providence, RI, 2003.
- [28] J. VON NEUMANN: *Discussion remark concerning paper of C.S. Smith “grain shapes and other metallurgical applications of topology”*, in: *Metal Interfaces*, American Society for Metals, American Society for Metals, Cleveland, Ohio, 1952, 108–110.

*Lavoro pervenuto alla redazione il 1 dicembre 2008
ed accettato per la pubblicazione il 2 febbraio 2009.
Bozze licenziate il 18 marzo 2009*

INDIRIZZO DEGLI AUTORI:

K. Barmak – Department of Materials Science and Engineering – Carnegie Mellon University – Pittsburgh, PA 15213

E-mail: katayun@andrew.cmu.edu

E. Eggeling – Fraunhofer Institut Computer Graphics Research IGD– Project Group Graz–A-8010 Austria

E-mail: eva.eggeling@fraunhofer.at

M. Emelianenko – Department of Mathematical Sciences – George Mason University – Fairfax, VA 22030

E-mail: memelian@gmu.edu

Y. Epshteyn – Department of Mathematical Sciences – Carnegie Mellon University – Pittsburgh, PA 15213

E-mail: rinal0@andrew.cmu.edu

D. Kinderlehrer – Department of Mathematical Sciences – Carnegie Mellon University – Pittsburgh, PA 15213

E-mail: davidk@cmu.edu

S. Ta’asan – Department of Mathematical Sciences – Carnegie Mellon University – Pittsburgh, PA 15213

E-mail: shlomo@andrew.cmu.edu